Natural atmospheric deposition of molybdenum: a global model and implications for tropical forests

As Published: https://doi.org/10.1007/s10533-020-00671-w

Publisher: Springer International Publishing

Persistent URL: https://hdl.handle.net/1721.1/131562

Version: Author's final manuscript: final author's manuscript post peer review, without publisher's formatting or copy editing

Natural atmospheric deposition of molybdenum: a global model and implications for tropical forests

Cite this article as: Michelle Y. Wong, Natalie M. Mahowald, Roxanne Marino, Earle R. Williams, Shankar Chellam and Robert W. Howarth, Natural atmospheric deposition of molybdenum: a global model and implications for tropical forests, Biogeochemistry https://doi.org/10.1007/s10533-020-00671-w

Running head

Atmospheric molybdenum deposition

Article type

Manuscript

Title

Natural atmospheric deposition of molybdenum: a global model and implications for tropical forests

Authors

Wong, Michelle Y.[1,2*], Natalie M. Mahowald[3], Roxanne Marino[1], Earle R. Williams[4], Shankar Chellam[5], Robert W. Howarth[1].

Affiliations

[1]Department of Ecology and Evolutionary Biology, Cornell University, Ithaca, NY 14853, U.S.A.

[2]Cary Institute of Ecosystem Studies, Millbrook, NY 12545, U.S.A.

[3]Department of Earth and Atmospheric Sciences, Cornell University, Ithaca, NY 14853, U.S.A.

[4]Massachusetts Institute of Technology, Cambridge, MA 02139, U.S.A.

[5]Department of Civil and Environmental Engineering, Texas A&M University, College Station, TX 77843, U.S.A.

*Corresponding Author: Dr. Michelle Wong; Cary Institute of Ecosystem Studies, Millbrook, NY, 12545, U.S.A.; telephone: (916) 833-0681; email: michelle.wong.ca@gmail.com

Key words

Atmospheric dust, sea-salt aerosols, Saharan dust, Sahel region, Bodélé Depression, Amazon Basin, tropical forests, nitrogen fixation

Abstract

Molybdenum (Mo) is an essential trace metal that plays a central role in biological nitrogen fixation (BNF) as the cofactor in the conventional form of the nitrogenase enzyme. The low availability of Mo in soils often constrains BNF in many terrestrial ecosystems. Atmospheric sources may supply a critical source of exogenous Mo to regions with highly weathered soils likely low in Mo, particularly in tropical forests where BNF is thought to be high. Here, we present results of a global model of Mo deposition that considers the principal natural sources of atmospheric Mo—windborne mineral dust, sea-salt aerosols, and volcanic sources—which operate over geologic time. The largest source of mineral dust globally is from North Africa. We

quantified Mo concentrations in dust and sediments from the Bodélé Depression, a large source within North Africa, to constrain our model. Because the Mo concentration of seawater is relatively high for a trace element, we also hypothesized that sea-salt aerosols would contribute atmospheric Mo. Our model predicts higher Mo deposition to terrestrial ecosystems along coasts downstream in trade winds, near active volcanoes, and in areas that receive dust deposition from North Africa, such as the northern Amazon Basin, the Caribbean, and Central America. Regions with higher Mo deposition tend to be areas where BNF has previously been measured. The lowest Mo deposition occurs in the high latitudes, northern parts of North America, Western Australia, Southern Africa, and much of central South America. Atmospheric transport of Mo likely plays an important role in supplying Mo to ecosystems across geologic time, particularly in regions with highly weathered soils.

Introduction

The distribution of molybdenum (Mo) deposition to terrestrial ecosystems from the atmosphere is important because Mo plays a critical role in biological nitrogen fixation (BNF), the reaction that transforms atmospheric nitrogen (N) into plant-available forms. Molybdenum is the most prevalent and efficient co-factor of the nitrogenase enzyme (Robson et al. 1986; Chi et al. 2009; Seefeldt et al. 2013; Mus et al. 2018), which catalyzes the reduction of dinitrogen (N_2) to ammonia (NH_3) and can be synthesized by all N-fixing organisms (Eady 1996). Mo limitation on BNF has been found in temperate, tropical, and boreal ecosystems (Barron et al. 2009; Wurzburger et al. 2012; Rousk et al. 2016; Perakis et al. 2017) and is considered to be the most common constraint on BNF across terrestrial ecosystems (Dynarski and Houlton 2018). Despite

the key biological role of Mo, it is rare in most soils, with an average crustal abundance of 1-2 μg g^{-1} (Taylor and McLennan 1995). Molybdenum availability is likely even lower across many acidic and highly weathered tropical soils remote from atmospheric inputs, where leaching over geologic time removes Mo and other soluble elements. Recent evidence has demonstrated that under extreme Mo deficiency, certain N-fixing organisms can synthesize "alternative" vanadium (V), and iron (Fe)-only nitrogenase isoforms can be utilized instead, with V or Fe in place of Mo as the co-factor (Zhang et al. 2016; McRose et al. 2017; Darnajoux et al. 2019). These non-Mo nitrogenases have a lower specific activity in laboratory experiments (Eady 1996) and may be less efficient for BNF, depending on constraints by metal availability under field conditions. As such, their significance in ecosystem-scale N inputs from BNF is not yet clear, particularly in the tropics where there has been no study of alternative nitrogenase activity. While there has been little study on Mo availability in tropical regions, Mo availability may be particularly low in remote regions such as the interior Amazon, where BNF has not yet been quantified, but rates are thought to be high (e.g. Wang and Houlton 2009) due to high rates of primary production and a high abundance trees that can form a symbiotic relationship with bacteria. Our current understanding of tropical BNF is geographically-limited, particularly for areas remote from the mineral dust, sea-salt aerosol, or volcanic inputs that provide the dominant natural sources for Mo deposition.

While weathering of parent material is the major contributor of rock-derived elements to soils, atmospheric deposition can be an important source of new nutrients to highly weathered soils (Chadwick et al. 1999). Sea-salt aerosols are carried inland varying distances by prevailing winds, and the largest rates of deposition occur in coastal regions. Because of sea-salt aerosol deposition, sodium (Na) concentrations in rainfall can drop up to 700-fold from coastal to inland

regions across 3000 km (Stallard and Edmond 1981). Molybdenum eventually leaches from soils into rivers and accumulates in the ocean owing to its high solubility when oxidized in the form of molybdate (MoO_4^{2-}). Because Mo is relatively unreactive in oxygenated, aqueous solution and is only very slowly removed from seawater by organisms or by most common mineral phases (Helz and Vorlicek 2019), Mo is the most abundant transition metal in the oceans. Since Mo is a conservative element in seawater (Manheim and Landergren 1978; Collier 1985; Nakagawa et al. 2012), Mo deposition from sea-salt aerosols follows the deposition pattern of Na and Cl, with highest deposition in coastal regions.

Away from coastal regions, mineral dust is the major source of aerosols globally, and annual estimates of dust production range from 1000-2150 Tg yr^{-1} (Zender et al. 2004). Dust aerosols are produced by wind erosion in arid and semi-arid regions, and the main source regions globally include the edges of the Sahara desert and Sahel region in North Africa (50-70% of global dust sources), the Arabian Peninsula, the Gobi and Taklamakan deserts in Asia (10-25%), and the Australian and South American deserts (Tegen and Schepanski 2009). The westward movement of North African dust across the Atlantic Ocean, and the presence of this dust in the Caribbean and the Amazon Basin are well-known (e.g. Artaxo et al. 1990). Dust from North Africa is thought to maintain long-term productivity of vegetation in the Amazon Basin (Swap et al. 1992; Okin et al. 2004; Yu et al. 2015) by supplying phosphorus (P). Although dust transport is highly variable from year to year, these dust emissions have likely occurred over tens of thousands of years (Albani et al. 2015a), and were possibly even higher before the Last Glacial Maximum (Mahowald et al. 1999) because of high aridity and wind speeds. A major portion of dust from the Sahara and Sahel regions comes from the Bodélé Depression in Chad (Koren et al. 2006), where the easily-eroded, diatomite-rich sediments are located between two mountain

chains that direct and accelerate the strong and frequent surface winds (Bristow et al. 2009). While the annual rates of dust deposition are typically low for most ecosystems when distributed over large areas, inputs of essential elements from this source can be important on geologic timescales (Swap et al. 1992; Chadwick et al. 1999). Empirical measurements and models have demonstrated that dust from North Africa are an important source of P and iron (Fe) in regions with P and Fe limitation and that North African dust weathers quickly and contributes to fertilization of the rainforest (Mahowald et al. 2005; Abouchami et al. 2013; Yu et al. 2015).

Volcanoes can also be a source of trace elements to the atmosphere when episodic events release volcanic ash composed of gases, aerosols, and metal salts. Even when not erupting, small amounts of sulfur dioxide gas leak from non-erupting degassing volcanoes, which act as carrier phases for trace elements. In volcanic aerosols from Kilauea volcano in Hawaii, Mo was relatively enriched compared with other trace elements (Sansone et al. 2002), indicating that volcanoes could also be a source for atmospheric Mo (King et al. 2016).

While estimates of total global sources of Mo to the atmosphere have been previously synthesized (Nriagu 1989), Mo deposition has not yet been estimated spatially. Differential deposition rates could influence ecosystem structure over geologic time. Model-based maps of deposition of Fe (Mahowald et al. 2005) and P (Mahowald et al. 2008) from different sources have been constructed, but Mo deposition has not yet been evaluated in a similar manner.

Here, we quantify for the first time Mo concentrations in mineral dust sources, and present the first model-based global deposition map for Mo. We focused on pre-industrial, natural source emissions with a particular emphasis on the fate of dust from the Sahara and Sahel regions and the potential impact of deposition on tropical regions such as the Amazon Basin. Previous studies based on precipitation concentrations and Mo isotopes indicate an important

role of atmospheric Mo in contributing to soil Mo (Marks et al. 2015; Siebert et al. 2015; King et al. 2016). Because anthropogenic activity has increased Mo deposition since the 19th century (Hong et al. 2004), biogenic particles and biomass burning could also be important modern sources of the atmospheric Mo cycle, redistributing local sources of Mo. In addition, catalyst manufacturing for chemical and petrochemical industries (Kulkarni et al. 2006), fossil fuel combustion (Cao et al. 2011), and traffic (Spada et al. 2012; Bozlaker et al. 2014), have led to enrichment of Mo in the atmosphere (Boonpeng et al. 2017; Dong et al. 2017). However, natural sources of sea-salt aerosols, mineral dust, and volcanoes likely dominated the atmospheric cycles during the past 12,000 years. Our objectives were to quantify Mo in dust, develop a model that depicts preindustrial atmospheric Mo deposition worldwide, and determine if these naturally occurring sources of Mo could be an important source of Mo to highly weathered soils of the world. Very low availability of Mo in such regions may constrain BNF, or favor activity by alternative nitrogenases. We hypothesized that: (1) dust inputs from North Africa are important to the northern Amazon, (2) sea-salt deposition is important only near coastal regions, and (3) that volcanoes could be locally important sources of Mo.

Methods

Sample collection

We obtained dried samples of dust and sediment (collected by E.R.W.) from the Bodélé Depression in September 2010 along the main trajectory of the wintertime Harmattan wind system, a dusty West African trade wind that moves westward from North Africa (see

Abouchami et al 2013 for details). The sediment samples consist of dry lake-bed sediments collected from eight locations approximately 200 km south of Faya Largeau, a town north of the Bodélé Depression. These sediments consist of mostly diatomites, the dominant material in the central lake bed of former Lake Megachad, which now is the Bodélé Depression. The five dust samples were collected from Chad and Niger from high ledges inside abandoned buildings in which dust had collected over a period of many decades. Sample locations and collections as well as data on many elements (but not Mo) are further described in Abouchami et al. (2013); sample names used in this paper are consistent with those in that reference (Table 1).

Sample analysis

Molybdenum concentrations in the dust and sediment samples were measured at the W.M. Keck Foundation Laboratory for Environmental Biogeochemistry, School of Earth & Space Exploration, Arizona State University (ASU). The dust and sediment samples were re-dried at 105°C, sieved at 2 mm and powdered, and ashed at 550°C overnight to remove organic matter. Samples were digested in HNO_3, HF, and HCl depending on sample solubility in a closed Savillex reactor on a hot plate. After digestion, samples were then diluted in 2% HNO_3 and Mo concentrations were determined by quadrupole ICP-MS (ThermoFisher Scientific iCAP Q, with CCT option). All samples were run in conjunction with SDO-1, a Devonian Ohio shale available from the USGS, and SCo-1, a grey shale low in Mo concentration available from the USGS, and yielded values of 142 ± 5.4 and 1.12 ± 0.2 µg g^{-1}, respectively (1 s.d.; n = 9).

Atmospheric modeling

To estimate natural Mo deposition from mineral dust, sea-salt aerosols, and volcanoes, we used an atmospheric transport model to simulate atmospheric Mo deposition from source areas through emission processes (Figure 1), transport, and deposition mechanisms using the parameterizations from Brahney et al. (2015). Because Mo in the atmosphere is present almost exclusively in the solid aerosol phase, we simulated Mo using an aerosol transport and deposition scheme within the Community Atmosphere Model, version 4 (CAM4), the atmospheric component of the Community Earth System Model (CESM) developed at the National Center for Atmospheric Research (NCAR). We ran the model using climate model-derived winds with the slab ocean model. Simulations were conducted for 5 years, with the last 4 years used for analysis. The model simulates three-dimensional transport and wet and dry deposition for gases and aerosols. Model spatial resolution was 1.9° by 2.5°. For each grid box, we obtained an estimate of deposition fluxes for every day of the year which were summed into annual estimates.

To model the Mo in sea-salt aerosols, we used a constant ratio of Mo to salinity in seawater used the sea-salt module (Mahowald et al. 2006) with parameterizations from Gong et al. (1997). Because Mo, unlike other biologically relevant trace elements, is conservative in seawater and maintains a constant ratio with salinity, the concentration of Mo in sea-salt aerosols reflects that of surface seawater (Manheim and Landergren 1978; Collier 1985). We derived the Mo sea-salt aerosol concentration from an average ocean Mo concentration of 106 nM (Collier 1985; Nakagawa et al. 2012) normalized to average salinity of 35 g salt kg^{-1} seawater, resulting in a value of 0.29 μg Mo g^{-1} salt. The source of the sea-salt aerosols was the open ocean under

high wind speed conditions (Figure 1a). Distribution into each size bin (0.1-1, 1-3, 3-10, and 10-20 μm) was independent of wind speed or relative humidity.

For Mo in dust, we assumed a constant fraction of the dust was Mo, using concentrations measured in this study (described above). In the model, mineral dust was entrained in unvegetated dry, arid regions with easily erodible soils during strong wind events. The dominant source regions of mineral aerosols were the arid regions of North Africa, the Arabian Peninsula, Central Asia, China, Australia, North America, and South Africa, most of which contain basins that drain from highlands that collect small particles (Figure 1b). The entrainment process to the atmosphere was proportional to the wind friction velocity, a measure of wind shear stress on soil surfaces and a function of planetary boundary layer winds, surface roughness, and atmospheric stability, further described by Mahowald et al. (2005b). The dust model included four particle size bins (0.1–1, 1–2.5, 2.5–5, and 5–10 μm) which were transported and deposited separately using the size fractionation by Albani et al. (2014). The regional source strengths of the mineral dusts were tuned to best match available aerosol optical depth, concentration and deposition data as described by Albani et al. (2014).

We used the Mo to sulfur (S) ratio to approximate volcanic Mo deposition, normalized to estimates of S emissions from volcanoes from gridded global data sets (Spiro et al. 1992) of non-erupting volcanoes (Figure 1c). Some of the major degassing volcanic regions include Vanuatu, Italy, Papua New Guinea, Colombia, Japan, Hawaii, Chile, Guatemala, and Nicaragua. Sulfur is used as a parameter for volcanic activity because of the ability to easily measure S with ground and satellite-based remote sensing (Carn et al. 2017). We simulated S emission as continuous release from active volcanoes. While volcanic ash from episodic events can contribute significant elements, we focused here on average estimated background volcanic activity for the

steady-state spatial model because of the difficulty in capturing historical episodic events, but included eruptive events in the total budget. We assumed that volcanic Mo is in fine aerosols because it is formed at high temperatures, and used a mass-based ratio of 4×10^{-4} of Mo/S from Nriagu (1989) to estimate Mo emissions as a fraction of S emissions. Volcanic aerosols were simulated in the size same bins as dust and sea salt for this study following Brahney et al. (2015). Once the aerosols were entrained into the atmosphere, they underwent transport, wet and turbulent dry depositions and gravitational settling appropriate for their assumed composition and size.

Sensitivity studies

In this study, we use model estimates of current, natural aerosol sources and deposition as typical for preindustrial values. Our modeled aerosols have been compared to available observations for the current climate (Mahowald et al. 2006; Liu et al. 2011; Albani et al. 2014). Preindustrial observations of aerosols are very limited (Carslaw et al. 2017) and based on ice core measurements in remote locations, far from the tropical regions. For dust, there are also very limited preindustrial measurements from marine, lake, and terrestrial sediments (Mahowald et al. 2010; Carslaw et al. 2017), which suggest an increase in current North African dust by about 40% (Mulitza et al. 2010; Mahowald et al. 2010). Because Mo deposition is likely important over the last 10-50,000 years, glacial, interglacial, and longer term fluctuations are important to consider. The dust records indicate large (~50%) decreases from North Africa seen in the mid-Holocene wet period (McGee et al. 2013; Albani et al. 2015b), but largely similar amounts from North Africa during both glacial and interglacial time periods (Maher et al. 2010; Albani et al.

2015b). Since desert dust deposition is thought to vary spatially by four to six orders of magnitude, and are thought to be uncertain to about a about a factor of ten, these factor of two fluctuations can be considered within the following sensitivity analysis. Sea-salt sources and deposition also vary by several orders of magnitude spatially and temporally (Mahowald et al., 2006) and have been measured in the ice cores, but these fluctuations are thought to be associated with sea ice formation, not necessarily sea-salt amounts (Wolff et al. 2003; Mahowald et al. 2006). Although it is possible that sea-salt fluxes change with temperature or winds, modeling studies suggest that these changes tend to be smaller than a factor of ten percent (Mahowald et al. 2006; Struthers et al. 2013), so again, the sensitivity analysis will include these bounds. There is no information about how non-explosive volcanoes might vary in the paleorecord.

We conducted a sensitivity analysis of deposition rates by increasing and decreasing rates uniformly by a factor calculated for each source. Using the variance formula to propagate error, we combined the largest factor of variation in ocean salinity (1.14) (Font et al. 2013) which causes variation in seawater Mo concentrations (Collier 1985), and largest factor of variation in dust and sediment Mo estimates (3.1) (this study), respectively, with an uncertainty of ten (described above) for a combined uncertainty factor of 10.1 for sea salts and 10.5 for dust. For volcanoes, we assumed an uncertainty value by a factor of ten.

$$u_{sea\ salt} = \sqrt{1.14^2 + 10^2} = 10.1$$

$$u_{dust} = \sqrt{3.1^2 + 10^2} = 10.5$$

We found this did not change the results qualitatively (Supplementary Information).

Observations

Atmospheric Mo is in the form of aerosols, but Mo is rarely measured on a routine basis due to its low concentrations (<1 ng m^{-3}), making detection and accurate quantification difficult. However, in urban areas near industrial sources, concentrations can range from 20-90 ng m^{-3} (Kuo et al. 2009; Na and Cocker, 2009). In this study, we are interested in long term (>10,000 years) Mo being transported in the atmosphere, so we looked for data where natural sources have dominated (Siebert et al. 2015). We also averaged measurements collected from Ragged Point, Barbados (13.165°N, 59.432°W), a source for North African dust deposition, collected between July and September 2013 and 2014. Methods are described in detail in (Bozlaker et al. 2018). Briefly, samples were collected on a 17 m scaffold tower with a high-volume system (1 m^3 min^{-1}) on 20 cm × 25 cm Whatman-41 (W-41) cellulose filters, digested using microwave digestion with combination of acids (HF, HNO_3, H_3BO_3, and sometimes also HCl), and analyzed for Mo using ICP-MS.

There are limited Mo datasets for deposition comparisons, both in general and in particular that are appropriate for preindustrial levels. We considered preindustrial ice core datasets, three of which include Mo measurements (Van de Velde et al. 1999; Hong et al. 2009; Sierra-Hernández et al. 2018), extracting ice concentration data and scaling up to deposition rates using ice accumulation rates when available, or best-estimates of precipitation.

Results

Dust Mo concentrations

The Bodélé Depression sediment Mo concentrations ranged from 0.7 to 3.6 μg g^{-1} and the Bodélé Depression dust Mo concentrations ranged from 1.0 to 1.3 μg g^{-1} (Table 1). The dust samples averaged a total Mo concentration of 1.15 ± 0.14 μg g^{-1} (1 s.d.) while the sediment samples averaged 1.42 ± 1.04 μg g^{-1}. The dust samples exhibited a much smaller range, likely due to filtering of particles that are entrained in the atmosphere and the downstream mixing that occurs in the atmosphere. We used the dust concentrations from this study to parameterize the model because up to half the dust from the Sahara, the main mineral source to the Amazon Basin, is thought to be emitted from the Bodélé Depression (Koren et al. 2006).

The average sediment and dust concentrations of 1.4 and 1.1 ug g^{-1} are within the range of the crustal abundance estimates of Mo at 1-2 μg g^{-1} (Taylor and McLennan 1995). Often modelers use the concentrations from crustal abundance when dust concentrations are not available (Chadwick et al. 1999; Okin et al. 2004); crustal abundance tends to give a conservative estimate for trace elements since dust is typically enriched in these elements (Lawrence and Neff 2009). Although we did not sample dust from other desert sources, the average concentration of dust measured from the Bodélé falls within the crustal abundance range; thus, we assume conservatively that the concentration of 1.1 μg Mo g^{-1} represents other mineral dust sources.

Modeled sea-salt deposition

Our model predicted higher Mo deposition from sea-salt aerosols in coastal regions facing trade winds (Figure 2a). Because of prevailing wind patterns in the equatorial regions where the

northeast and southeast trade winds converge, the Caribbean and the northeast coast of South America received relatively high Mo deposition compared to the islands situated between the Indian and Pacific Oceans. Deposition rates were higher and extended farther inland to terrestrial ecosystems in the coastal regions of western North America, Western Europe, southern Asia, eastern South America, eastern and southern Australia, Hawaiian Islands, and Central America. The East Indies, eastern North America, western South America, and northwestern Australia, which do not have onshore trade winds, received less sea-salt-derived Mo deposition. Because of higher wind speeds in the latitudinal regions, sea-salt sources and subsequent deposition rates were generally higher across the oceans farther from the equator. In South America, for example, moving westward, there was a drop-off of sea-salt aerosol deposition rates. Near Maceio, Brazil at 10.4°S and 35°W, sea-salt deposition rates abruptly declined from 6 μg Mo m^{-2} yr^{-1} by 58% across 270 km, by 90% across 820 km, and by 94% across 1400 km (Figure 2a).

Modeled Mo dust deposition

The regions that received the most Mo from mineral dust were proximal to the dust sources with onshore winds, such as North Africa, the Arabian Peninsula, the Gobi and Taklamakan deserts in Asia, deserts in central and southern Australia, the Patagonian desert in the southern part of South America, and the southwestern U.S (Figure 2b). For example, following the westerly winds, dust moved eastward from the Gobi and Taklamakan deserts in Asia. Exogenous deposition rates were highest, similar to sea-salt spray, in the direction following trade wind movement. Globally, the highest rates decreased moving westward from North Africa, as dust from that source is deposited in the Caribbean, Central America, and the northern Amazon

Basin. We found a particularly steep gradient in Mo dust deposition from northern South America to central South America (Figure 2b). For example, moving south from Trindad and Tobago in the Caribbean, dust deposition rates decreased from a peak at 8.5°N and 60°W from 30 μg Mo m^{-2} yr^{-1} to 4.2 μg Mo m^{-2} yr^{-1} at 2.38°S and 60°W near Manaus, Brazil in the Amazon. This pattern held relatively constant from the northern to southern Amazon Basin.

Modeled Mo volcano deposition

The major volcanic sources of Mo were located near the major degassing volcanic regions, such as active volcanoes in Italy, Papua New Guinea, Colombia, Japan, Hawaii, Chile, Guatemala, and Nicaragua (Carn et al. 2017). Volcanic Mo deposition decreased with distance from the source along the trajectory of trade winds. We found the highest deposition rates in Papua New Guinea at 16 μg Mo m^{-2} yr^{-1}. Within the Hawaiian Islands, the highest deposition rates were 1.5 μg Mo m^{-2} yr^{-1} near the island of Hawai'i, and values dropped off three-fold to nearby Hawaiian Islands due to scavenging by precipitation, such as on Kauai, located 500 km away. Deposition associated with volcanic activity ranged from 0.1 to 10 μg Mo m^{-2} yr^{-1} across Central America and the Andean region, and from 0.1 to 5 μg Mo m^{-2} yr^{-1} from central Chile to the southern parts of South America (Figure 2c).

Total modeled Mo deposition

When combining sea-salt, dust, and volcanic aerosol deposition, we estimate the lowest rates of preindustrial, natural Mo deposition in the northern parts of North America, the Indian Ocean,

Western Australia, Southern Africa, and much of central South America and the southern tip of South America, and the polar regions (Figure 2d). In the central part of South America, for example, at 65°W and 29.4°S, total deposition rates were 0.46 μg Mo m^{-2} yr^{-1}. The total deposition patterns followed the dust and sea-salt deposition patterns closely, with the highest deposition rates (up to 1200 μg Mo m^{-2} yr^{-1}) near dust sources and downwind of dust sources, coastal regions facing trade winds, and near active degassing volcanoes (Figure 2d).

Mineral dust inputs to the atmosphere dominated natural sources of Mo (70%) and sea-salt aerosols followed (26%), while the smallest sources were degassing and eruptive volcanoes (4%) (Table 2). Dust deposition had a far-reaching influence on terrestrial land surfaces within the same continent as the source regions, but also across oceans. Sea-salt aerosols were the second largest source of natural aerosols, with the highest deposition rates occurring in coastal regions facing trade winds. Volcanoes were the smallest source globally, and had predominantly local influences near active, degassing volcanoes. In tropical regions with low dust and sea-salt deposition such as Indonesia, volcanic sources dominated. Across most tropical regions, either dust, sea-salt aerosols, or volcanic activity contributed notable amounts of atmospheric Mo deposition, except for the central region of South America. For example, Hawaii and Central America received between 1 and 50 μg Mo m^{-2} yr^{-1}, the northern Amazon received between 1 to 10 μg Mo m^{-2} yr^{-1}, and the southern Amazon received between 0.1 to 1 μg Mo m^{-2} yr^{-1}. It is notable that many of the regions where BNF has been measured in the tropics are located in areas with higher rates of sea-salt Mo deposition (Figure 2d), such as the Hawaiian Islands, Central America, and coastal South America.

Discussion

Our model results suggest that globally, mineral dust inputs dominate the natural atmospheric cycle (Table 2). Our estimates are some three-fold higher for dust, eight-fold higher for sea-salt aerosols, and roughly half as much for volcanoes compared to previous estimates (Nriagu 1989). Nriagu's sea-salt aerosol and dust estimates were lower because they normalized their sea-salt production to 0.1-1 x 10^{16} g of sea-salt spray and their dust production to 0.6 to 5 x 10^{14} g of dust derived from Prospero et al. (1983), while our estimates are derived from simulated sea-salt aerosol and dust entrainment into the atmosphere that were previously tuned to observational data (Mahowald et al. 2006, 2008). Our modeled estimates for sea-salt aerosol Mo deposition are relatively robust because the model estimates were previously tuned to empirical measurements of Na and chloride for sea-salt aerosols (Mahowald et al. 2008), and the highly conservative nature of Mo leads to a consistent ratio with sea salts. Our mineral dust model is relatively robust as well, because the dust model has been tuned to observational data from aerosols and satellite data (Mahowald 2003). Although we parameterized the model with dust samples from the Bodélé Depression, the concentrations from this region fit within the crustal abundance range and represents the largest global source relative to its size. The least well-constrained estimates are the volcano sources because we used a Mo/S ratio, and Mo is rarely measured in volcano plumes or in volcanic ash (Crowe et al. 1987), and often not together with S (e.g. Mather et al. 2012). Our estimates of volcanic emissions from active, degassing volcanoes are likely on the higher end, since Mo is much less volatile than S. While trace metals are often thought to be abundant in degassing volcano plumes because of fractionation processes that concentrate trace metals (Hinkley et al. 1994), a study conducted in Iceland demonstrated relatively low levels of

Mo in degassing materials (Arnórsson and Óskarsson 2007). Though volatilization of Mo from degassing volcanoes still needs to be investigated, eruptive volcanoes are still likely a source of Mo, as in Hawaii, where Mo in soils was isotopically traced to volcanic emissions (King et al. 2016).

As discussed in the description of the sensitivity studies above, there is a large uncertainty in the deposition of Mo because 1) natural aerosols in preindustrial and over glacial and interglacial time scales are poorly constrained by observations, and 2) because of uncertainties in the Mo composition of these aerosols (Carslaw et al. 2017; Albani et al. 2018). However, sensitivity studies suggest that these uncertainties do not qualitatively change our results. While the model cannot be well-validated with current observational data due to the paucity of field measurements and the potential for anthropogenic influence, we compared model estimates with three preindustrial ice core measurements of Mo, an empirical estimate of atmospheric Mo deposition based on precipitation fluxes, and monthly measurements from Barbados, areas likely less influenced by anthropogenic Mo (Supplementary Table S3) (Siebert et al. 2015; Bozlaker et al. 2018). Modeled and observed deposition estimates from ice core data in Mount Everest and Mont Blanc were closely aligned (10.5 μg Mo m^{-2} yr^{-1}, modeled, vs. 6.9 μg Mo m^{-2} yr^{-1}, observed at Mount Everest; and 11.9 μg Mo m^{-2} yr^{-1}, modeled, vs. 10.8 μg Mo m^{-2} yr^{-1}, observed for Mont Blanc) (Van de Velde et al. 1999; Hong et al. 2009), while the model over predicted Mo deposition in the northwestern Tibetan Plateau (31.2 Mo μg m^{-2} yr^{-1}, modeled, vs. a mean of 5.2 and range from 0.5 to 40 μg Mo m^{-2} yr^{-1}, observed) (Sierra-Hernández et al. 2018). In Iceland, where we expect sea-salt deposition to dominate, and Barbados, where we expect dust deposition to dominate, the modeled and the modern observed estimates were within the same order of magnitude (Supplementary Table S1), although observed estimates were

always higher. Measured estimates of Mo were over two-fold higher in Barbados, likely due to a higher estimate of dust, demonstrated by the two-fold higher estimate of Al, a proxy for dust (e.g. Bozlaker et al. 2018). Previous model-data comparison studies of dust deposition and concentrations show the difficulty of correctly simulating the emission, long range transport and deposition of natural aerosols like desert dust (Huneeus et al. 2011), so an uncertainty by a factor of ten in dust distributions and deposition is common (Huneeus et al. 2011; Mahowald et al. 2011). Because we expect the sources and deposition of dust and sea salts, the most important natural sources of Mo, to vary by four to six orders of magnitude spatially on an annual average (e.g. Albani et al., 2015; Figures 1 and 2), estimates within one order of magnitude still capture most of the spatial variability.

Across long timescales, atmospheric Mo deposition could support Mo cycling in ecosystems that receive relatively high Mo atmospheric deposition with low weathering of parent material. For example, in Iceland where sea-salt aerosol deposition is relatively high, Siebert et al. (2015) suggested that atmospheric deposition contributed to between 5 and 9% of the soil Mo pool relative to the basaltic bedrock. They found the strongest sea-salt influence (9%) in the more weathered soils (Siebert et al. 2015). These results suggest that atmospheric Mo inputs can be particularly important in older, highly weathered soils in regions of high precipitation, where soluble Mo has been lost to leaching. Strong evidence that soil age affects rock-derived nutrient availability also comes from Hawaiian Islands, which vary widely in ecosystem age, ranging from 300 to 4,100,000 years old. Atmospheric P and calcium (Ca) inputs are particularly important for the fertility of the older islands, where the basaltic parent material is highly weathered. On islands older than 20,000 years, atmospheric inputs of Ca are the dominant source of this element (Chadwick et al. 1999). Hawaii is a region where sea-salt deposition of Mo and

volcanic deposition of Mo are relatively high, and where BNF rates have also been found to be high (Vitousek and Walker 1989; Ley and D'Antonio 1998; Pearson and Vitousek 2002). The important role of atmospheric Ca suggests that atmospheric Mo may also be important to the older islands, potentially supplying Mo to sustain BNF and prevent Mo limitation of BNF (Hobbie and Vitousek 2000).

Although tropical forests are often situated on highly weathered soils, they are thought to be major global sites of BNF (Cleveland et al. 1999; Wang and Houlton 2009) for a few reasons. First, tropical forests have a higher abundance of leguminous trees capable of forming symbiotic relationships with bacteria compared to other biomes. Second, the warm, wet conditions of the litter layer facilitate higher rates of heterotrophic, free-living BNF catalyzed by bacteria and archaea. In addition, higher BNF rates in the tropics have been associated with the canopy, epiphytes, decaying wood, bryophytes, and lichens compared to other ecosystems (Cleveland et al. 1999; Matzek and Vitousek 2003). However, evidence of Mo limitation on BNF in tropical forests and other biomes has been increasing (Dynarski and Houlton 2018). Phosphorus was previously thought to be the dominant nutrient control on BNF, but teasing apart the effects of Mo and P in previous research is complicated. In many P addition experiments, Mo may have been present as a contaminant, calling into question the results of historical experiments with P addition where Mo could have been inadvertently added (Barron et al. 2009). Almost all previous addition experiments in different biomes have demonstrated Mo limitation on BNF to some extent. However, much of the previous research on Mo and its control on BNF, measured through Mo fertilization experiments, has been conducted in regions where atmospheric deposition of Mo may supply sufficient Mo to support BNF (Figure 3). Even where atmospheric Mo deposition is relatively high in tropical forests in Panama, previous addition experiments

have demonstrated an experimental response of free-living BNF to Mo at rates of 39 μg m^{-2} yr^{-1} (Barron et al. 2009). Additionally, canopy BNF, which is highly sensitive to atmospheric inputs, in Panama has also been found to be influenced by Mo availability (Stanton et al. 2019). According to our model, Mo could be supplied by atmospheric deposition, depending on the region, over decades to hundreds of years in some tropical regions (Figure 2d).

Thus, if Mo availability constrains BNF widely across tropical forests, then this constraint is likely more prominent in N-limited regions of low Mo deposition where parent material weathering is also low. For example, the eastern, central and southeastern Amazon are some of the oldest geologic surfaces exposed in South America, with maximum geological ages ranging from 1500 to 3600 million years (Quesada et al. 2011). In the Amazon, the lack of recent geologic activity has suggested the link of atmospheric inputs of P with the long-term productivity of the forests (Swap et al. 1992). Okin et al. (2004) speculated that in the Amazon and Congo Basins, dust P inputs from the Sahara are large enough relative to soil concentrations to have replenished the soil P many times since the evolution of these ecosystems. From isotopic analysis, the lack of strong dust accumulation from the Bodélé in the Amazon Basin suggests that the dust is consumed, potentially contributing nutrients, including trace elements like Mo, to stimulate plant growth (Abouchami et al. 2013). While there are not adequate soil Mo measurements across the Amazon and Congo Basins to make the same conclusion as Okin et al. (2004) did for P, their results, along with our modeled deposition rates, suggest that Mo availability could be relatively low across the lower Amazon and could constrain BNF, compared to other regions like Hawaii where BNF rates have been measured to be relatively high, and Mo deposition is also relatively high (Figure 2d). Because interior regions of the

Amazon with low natural Mo deposition are understudied, BNF may be more limited by Mo in these regions.

The genes for alternative nitrogenases are sometimes present in free-living N fixers, but always co-occur with the Mo nitrogenase. In experimental pure culture studies, the absence of Mo causes alternative nitrogenase activity to increase, suggesting that alternative nitrogenases can sustain BNF when Mo availability is low. While alternative nitrogenase genes have been found in many ecosystems (Betancourt et al. 2008; McRose et al. 2017), their activity has only been measured in two studies (Zhang et al. 2016; Darnajoux et al. 2019), including a boreal forest where both atmospheric and bedrock inputs of Mo are low (Darnajoux et al. 2019). Thus, some of the areas we highlight with very low Mo deposition and that also have highly Mo-depleted soils may also be areas where alternative nitrogenase activity could be important. Thus we highly encourage more studies of BNF in these regions, because 1) BNF rates may be lower than modeled estimates and/or 2), these may be areas where alternative nitrogenases may play an important role.

Here, we demonstrate the large range, up to six orders of magnitude, in deposition rates of atmospheric Mo globally, which could impact ecosystem structure and function, particularly in N-limited ecosystems. To better quantify the importance of atmospheric Mo, we need to further understand the retention and loss of Mo within ecosystems, collect more empirical observations of Mo in soils and aerosols, and study the impacts of human activity and land-use change on the atmospheric Mo cycle. This will help elucidate how tightly coupled Mo availability will likely be to atmospheric Mo transport in the future, and what the ultimate impact of atmospheric Mo on N cycling is. Finally, to better understand controls on BNF, BNF should

be measured in more remote tropical forests, many of which receive little to no atmospheric Mo inputs, and could be limited by Mo.

Acknowledgements

We thank Gwyneth W. Gordon and Ariel D. Anbar at ASU for help with the analysis of the dust and sediment samples, and Tim Fahey and Christopher Neill for comments on the manuscript. This work was funded by a grant from the David R. Atkinson Center for a Sustainable Future to R.W.H, R.M., N.M.M., and Murray McBride. M.Y.W. was supported by an NSF IGERT Fellowship and an NSF Graduate Research Fellowship.

References

Abouchami W, Näthe K, Kumar A, et al (2013) Geochemical and isotopic characterization of the Bodélé Depression dust source and implications for transatlantic dust transport to the Amazon Basin. Earth Planet Sci Lett 380:112–123. https://doi.org/10.1016/j.epsl.2013.08.028

Albani S, Balkanski Y, Mahowald N, et al (2018) Aerosol-Climate Interactions During the Last Glacial Maximum. Curr Clim Chang Reports 4:99–114. https://doi.org/10.1007/s40641-018-0100-7

Albani S, Mahowald NM, Perry AT, et al (2014) Improved dust representation in the Community Atmosphere Model. J Adv Model Earth Syst 6:541–570. https://doi.org/10.1002/2013MS000279

Albani S, Mahowald NM, Winckler G, et al (2015a) Twelve thousand years of dust: The Holocene global dust cycle constrained by natural archives. Clim Past 11:869–903.

https://doi.org/10.5194/cp-11-869-2015

Albani S, Mahowald NM, Winckler G, et al (2015b) Tweleve thousand years of dust: the Holocene global dust cycle constrained by natural archives. Clim Past 11:869–2015. https://doi.org/10.5194/cp-11-869-2015

Arnórsson S, Óskarsson N (2007) Molybdenum and tungsten in volcanic rocks and in surface and <100 °C ground waters in Iceland. Geochim Cosmochim Acta 71:284–304. https://doi.org/10.1016/j.gca.2006.09.030

Artaxo P, Maenhaut W, Storms H, Van Grieken R (1990) Aerosol characteristics and sources for the Amazon Basin during the wet season. J Geophys Res 95:16971–16985. https://doi.org/10.1029/JD095iD10p16971

Barron AR, Wurzburger N, Bellenger JP, et al (2009) Molybdenum limitation of asymbiotic nitrogen fixation in tropical forest soils. Nat Geosci 2:42–45. https://doi.org/10.1038/ngeo366

Betancourt DA, Loveless TM, Brown JW, Bishop PE (2008) Characterization of diazotrophs containing Mo-independent nitrogenases, isolated from diverse natural environments. Appl Environ Microbiol 74:3471–3480. https://doi.org/10.1128/AEM.02694-07

Boonpeng C, Polyiam W, Sriviboon C, et al (2017) Airborne trace elements near a petrochemical industrial complex in Thailand assessed by the lichen Parmotrema tinctorum (Despr. ex Nyl.) Hale. Environ Sci Pollut Res 24:12393–12404. https://doi.org/10.1007/s11356-017-8893-9

Bozlaker A, Prospero JM, Price J, Chellam S (2018) Linking Barbados Mineral Dust Aerosols to North African Sources Using Elemental Composition and Radiogenic Sr, Nd, and Pb Isotope Signatures. J Geophys Res Atmos 123:1384–1400.

https://doi.org/10.1002/2017JD027505

Bozlaker A, Spada NJ, Fraser MP, Chellam S (2014) Elemental characterization of $PM_{2.5}$ and PM_{10} emitted from light duty vehicles in the Washburn Tunnel of Houston, Texas: Release of rhodium, palladium, and platinum. Environ Sci Technol 48:54–62. https://doi.org/10.1021/es4031003

Brahney J, Mahowald N, Ward DS, et al (2015) Is atmospheric phosphorus pollution altering global alpine Lake stoichiometry? Global Biogeochem Cycles 29:1369–1383. https://doi.org/10.1002/2015GB005137

Bristow CS, Drake N, Armitage S (2009) Deflation in the dustiest place on Earth: The Bodélé Depression, Chad. Geomorphology 105:50–58. https://doi.org/10.1016/j.geomorph.2007.12.014

Cao Z, Yang Y, Lu J, Zhang C (2011) Atmospheric particle characterization, distribution, and deposition in Xi'an, Shaanxi Province, Central China. Environ Pollut 159:577–584. https://doi.org/10.1016/j.envpol.2010.10.006

Carn SA, Fioletov VE, Mclinden CA, et al (2017) A decade of global volcanic SO_2 emissions measured from space. Sci Rep 7:1–12. https://doi.org/10.1038/srep44095

Carslaw KS, Gordon H, Hamilton DS, et al (2017) Aerosols in the Pre-industrial Atmosphere. Curr Clim Chang Reports 3:1–15. https://doi.org/10.1007/s40641-017-0061-2

Chadwick OA, Derry LA, Vitousek PM, et al (1999) Changing sources of nutrients during four million years of ecosystem development. Nature 397:491–497. https://doi.org/10.1038/17276

Chi CL, Hu Y, Ribbe MW (2009) Unique features of the nitrogenase VFe protein from Azotobacter vinelandii. Proc Natl Acad Sci U S A 106:9209–9214.

https://doi.org/10.1073/pnas.0904408106

Cleveland CC, Townsend AR, Schimel DS, et al (1999) Global patterns of terrestrial biological nitrogen (N_2) fixation in natural ecosystems. Global Biogeochem Cycles 13:623–645. https://doi.org/10.1029/1999GB900014

Collier RW (1985) Molybdenum in the Northeast Pacific Ocean. Limnol Oceanogr 30:1351–1354. https://doi.org/10.4319/lo.1985.30.6.1351

Crowe BM, Finnegan DL, Zoller WH, Boynton W V. (1987) Trace element geochemistry of volcanic gases and particles from 1983-1984 eruptive episodes of Kilauea Volcano. J Geophys Res Solid Earth 92:13708–13714. https://doi.org/10.1029/jb092ib13p13708

Darnajoux R, Magain N, Renaudin M, et al (2019) Molybdenum threshold for ecosystem scale alternative vanadium nitrogenase activity in boreal forests. Proc Natl Acad Sci 116:201913314. https://doi.org/10.1073/pnas.1913314116

Dong Z, Qin D, Qin X, et al (2017) Changes in precipitating snow chemistry with seasonality in the remote Laohugou glacier basin, western Qilian Mountains. Environ Sci Pollut Res 24:11404–11414. https://doi.org/10.1007/s11356-017-8778-y

Dynarski KA, Houlton BZ (2018) Nutrient limitation of terrestrial free-living nitrogen fixation. New Phytol 217:1050–1061. https://doi.org/10.1111/nph.14905

Eady RR (1996) Structure−function relationships of alternative nitrogenases. Chem Rev 96:3013–3030. https://doi.org/10.1021/cr950057h

Font J, Boutin J, Reul N, et al (2013) SMOS first data analysis for sea surface salinity determination. Int J Remote Sens 34:3654–3670. https://doi.org/10.1080/01431161.2012.716541

Gong SL, Barrie LA, Blanchet J-P (1997) Modeling sea-salt aerosols in the atmosphere: 1.

Model development. J Geophys Res Atmos 102:3805–3818. https://doi.org/10.1029/96JD02953

Helz GR, Vorlicek TP (2019) Precipitation of molybdenum from euxinic waters and the role of organic matter. Chem Geol 509:178–193. https://doi.org/10.1016/j.chemgeo.2019.02.001

Hinkley TK, Le Cloarec MF, Lambert G (1994) Fractionation of families of major, minor, and trace metals across the melt-vapor interface in volcanic exhalations. Geochim Cosmochim Acta 58:3255–3263. https://doi.org/10.1016/0016-7037(94)90053-1

Hobbie SE, Vitousek PM (2000) Nutrient limitation of decomposition in hawaiian forests. Ecology 81:1867–1877. https://doi.org/10.1890/0012-9658(2000)081[1867:NLODIH]2.0.CO;2

Hong S, Barbante C, Boutron C, et al (2004) Atmospheric heavy metals in tropical South America during the past 22,000 years recorded in a high altitude ice core from Sajama, Bolivia. J Environ Monit 6:322–326. https://doi.org/10.1039/b314251e

Hong S, Lee K, Hou S, et al (2009) An 800-year record of atmospheric As, Mo, Sn, and Sb in central Asia in high-altitude ice cores from Mt. Qomolangma (Everest), Himalayas. Environ Sci Technol 43:8060–8065. https://doi.org/10.1021/es901685u

Huneeus N, Schulz M, Balkanski Y, et al (2011) Global dust model intercomparison in AeroCom phase I. Atmos Chem Phys 11:7781–7816. https://doi.org/10.5194/acp-11-7781-2011

King EK, Thompson A, Chadwick OA, Pett-Ridge JC (2016) Molybdenum sources and isotopic composition during early stages of pedogenesis along a basaltic climate transect. Chem Geol 445:54–67. https://doi.org/10.1016/j.chemgeo.2016.01.024

Koren I, Kaufman YJ, Washington R, et al (2006) The Bodélé depression-a single spot in the

Sahara that provides most of the mineral dust to the Amazon forest. Environ Res Lett 1:1–5. https://doi.org/10.1088/1748-9326/1/1/014005

Kulkarni P, Chellam S, Fraser MP (2006) Lanthanum and lanthanides in atmospheric fine particles and their apportionment to refinery and petrochemical operations in Houston, TX. Atmos Environ 40:508–520. https://doi.org/10.1016/j.atmosenv.2005.09.063

Kuo CY, Wang JY, Chang SH, Chen MC (2009) Study of metal concentrations in the environment near diesel transport routes. Atmos Environ 43:3070–3076. https://doi.org/10.1016/j.atmosenv.2009.03.028

Lawrence CR, Neff JC (2009) The contemporary physical and chemical flux of aeolian dust: A synthesis of direct measurements of dust deposition. Chem Geol 267:46–63. https://doi.org/10.1016/j.chemgeo.2009.02.005

Ley RE, D'Antonio CM (1998) Exotic grass invasion alters potential rates of N fixation in Hawaiian woodlands. Oecologia 113:179–187. https://doi.org/10.1007/s004420050366

Liu X, Easter RC, Ghan SJ, et al (2011) Toward a minimal representation of aerosol direct and indirect effects: model description and evaluation. Geosci Model Dev Discuss 4:3485–3598. https://doi.org/10.5194/gmdd-4-3485-2011

Maher BA, Prospero JM, Mackie D, et al (2010) Global connections between aeolian dust, climate and ocean biogeochemistry at the present day and at the last glacial maximum. Earth-Science Rev 99:61–97. https://doi.org/10.1016/j.earscirev.2009.12.001

Mahowald N (2003) Interannual variability in atmospheric mineral aerosols from a 22-year model simulation and observational data. J Geophys Res 108:4352. https://doi.org/10.1029/2002JD002821

Mahowald N, Albani S, Engelstaedter S, et al (2011) Model insight into glacial-interglacial

paleodust records. Quat Sci Rev 30:. https://doi.org/10.1016/j.quascirev.2010.09.007

Mahowald N, Jickells TD, Baker AR, et al (2008) Global distribution of atmospheric phosphorus sources, concentrations and deposition rates, and anthropogenic impacts. Global Biogeochem Cycles 22:. https://doi.org/10.1029/2008GB003240

Mahowald N, Kohfeld K, Hansson M, et al (1999) Dust sources and deposition during the last glacial maximum and current climate: A comparison of model results with paleodata from ice cores and marine sediments. J Geophys Res Atmos 104:15895–15916. https://doi.org/10.1029/1999JD900084

Mahowald NM, Baker AR, Bergametti G, et al (2005) Atmospheric global dust cycle and iron inputs to the ocean. Global Biogeochem Cycles 19:1–15. https://doi.org/10.1029/2004GB002402

Mahowald NM, Kloster S, Engelstaedter S, et al (2010) Observed 20th century desert dust variability: impact on climate and biogeochemistry. Atmos Chem Phys 10:10875–10893. https://doi.org/10.5194/acp-10-10875-2010

Mahowald NM, Lamarque J-F, Tie XX, Wolff E (2006) Sea-salt aerosol response to climate change: Last Glacial Maximum, preindustrial, and doubled carbon dioxide climates. J Geophys Res Atmos 111:. https://doi.org/10.1029/2005JD006459

Manheim FT, Landergren S (1978) Molybdenum. In: Handbook of Geochemistry. p V. II/5, Sections 42 BO.

Marks JA, Perakis SS, King EK, Pett-Ridge J (2015) Soil organic matter regulates molybdenum storage and mobility in forests. Biogeochemistry 125:167–183. https://doi.org/10.1007/s10533-015-0121-4

Mather TA, Witt MLI, Pyle DM, et al (2012) Halogens and trace metal emissions from the

ongoing 2008 summit eruption of Kilauea volcano, Hawai'i. Geochim Cosmochim Acta 83:292–323. https://doi.org/10.1016/j.gca.2011.11.029

Matzek V, Vitousek P (2003) Nitrogen fixation in bryophytes, lichens, and decaying wood along a soil-age gradient in Hawaiian montane rain forest. Biotropica 35:12–19. https://doi.org/10.1111/j.1744-7429.2003.tb00257.x

McGee D, deMenocal P, Winckler G, et al (2013) The magnitude, timing and abruptness of changes in North African dust deposition over the last 20,000 yr. Earth Planet Sci Lett 371–273:163–176

McRose DL, Zhang X, Kraepiel AML, Morel FMM (2017) Diversity and activity of alternative nitrogenases in sequenced genomes and coastal environments. Front Microbiol 8:1–13. https://doi.org/10.3389/fmicb.2017.00267

Mulitza S, Heslop D, Pittauerova D, et al (2010) Increase in African dust flux at the onset of commercial agriculture in the Sahel region. Nature 466:226–228. https://doi.org/10.1038/nature09213

Mus F, Alleman AB, Pence N, et al (2018) Exploring the alternatives of biological nitrogen fixation. Metallomics 10:523–538. https://doi.org/10.1039/c8mt00038g

Na K, Cocker DR (2009) Characterization and source identification of trace elements in PM2.5 from Mira Loma, Southern California. Atmos Res 93:793–800. https://doi.org/10.1016/j.atmosres.2009.03.012

Nakagawa Y, Takano S, Firdaus M (2012) The molybdenum isotopic composition of the modern ocean. Geochem J 46:131–141. https://doi.org/10.2343/geochemj.1.0158

Nriagu JO (1989) A global assessment of natural sources of atmospheric trace metals. Nature 338:47–49. https://doi.org/10.1038/338047a0

Okin GS, Mahowald N, Chadwick OA, Artaxo P (2004) Impact of desert dust on the biogeochemistry of phosphorus in terrestrial ecosystems. Global Biogeochem Cycles 18:. https://doi.org/10.1029/2003GB002145

Pearson HL, Vitousek PM (2002) Soil phosphorus fractions and symbiotic nitrogen fixation across a substrate-age gradient in Hawaii. Ecosystems 5:587–596. https://doi.org/10.1007/s10021-002-0172-y

Perakis SS, Pett-Ridge JC, Catricala CE (2017) Nutrient feedbacks to soil heterotrophic nitrogen fixation in forests. Biogeochemistry 134:41–55. https://doi.org/10.1007/s10533-017-0341-x

Prospero JM, Charlson RJ, Mohnen V, et al (1983) The atmospheric aerosol system: an overview. Rev Geophys Sp Phys 21:1607–1629. https://doi.org/10.1029/RG021i007p01607

Quesada CA, Lloyd J, Anderson LO, et al (2011) Soils of Amazonia with particular reference to the RAINFOR sites. Biogeosciences 8:1415–1440. https://doi.org/10.5194/bg-8-1415-2011

Robson RL, Eady RR, Richardson TH, et al (1986) The alternative nitrogenase of Azotobacter chroococcum is a vanadium enzyme. Nature 322:388–390. https://doi.org/10.1038/322388a0

Rousk K, Degboe J, Michelsen A, et al (2016) Molybdenum and phosphorus limitation of moss-associated nitrogen fixation in boreal ecosystems. New Phytol 214:97–107. https://doi.org/10.1111/nph.14331

Sansone FJ, Benitez-Nelson CR, Resing JA, et al (2002) Geochemistry of atmospheric aerosols generated from lava-seawater interactions. Geophys Res Lett 29:49-1-49–4. https://doi.org/10.1029/2001GL013882

Seefeldt LC, Yang ZY, Duval S, Dean DR (2013) Nitrogenase reduction of carbon-containing compounds. Biochim Biophys Acta - Bioenerg 1827:1102–1111.

https://doi.org/10.1016/j.bbabio.2013.04.003

Siebert C, Pett-Ridge JC, Opfergelt S, et al (2015) Molybdenum isotope fractionation in soils: Influence of redox conditions, organic matter, and atmospheric inputs. Geochim Cosmochim Acta 162:1–24. https://doi.org/10.1016/j.gca.2015.04.007

Sierra-Hernández MR, Gabrielli P, Beaudon E, et al (2018) Atmospheric depositions of natural and anthropogenic trace elements on the Guliya ice cap (northwestern Tibetan Plateau) during the last 340 years. Atmos Environ 176:91–102. https://doi.org/10.1016/j.atmosenv.2017.11.040

Spada N, Bozlaker A, Chellam S (2012) Multi-elemental characterization of tunnel and road dusts in Houston, Texas using dynamic reaction cell-quadrupole-inductively coupled plasma-mass spectrometry: Evidence for the release of platinum group and anthropogenic metals from motor vehicles. Anal Chim Acta 735:1–8. https://doi.org/10.1016/j.aca.2012.05.026

Spiro PA, Jacob DJ, Logan JA (1992) Global inventory of sulfur emissions with 1° × 1° resolution. J Geophys Res 97:6023–6036. https://doi.org/10.1029/91JD03139

Stallard RF, Edmond JM (1981) Geochemistry of the Amazon: 1. Precipitation chemistry and the marine contribution to the dissolved load at the time of peak discharge. J Geophys Res 86:9844–9858. https://doi.org/10.1029/JC086iC10p09844

Stanton DE, Batterman SA, Von Fischer JC, Hedin LO (2019) Rapid nitrogen fixation by canopy microbiome in tropical forest determined by both phosphorus and molybdenum. Ecology 100:1–8. https://doi.org/10.1002/ecy.2795

Struthers H, Ekman AML, Glantz P, et al (2013) Climate-induced changes in sea salt aerosol number emissions: 1870 to 2100. J Geophys Res Atmos 118:670–682.

https://doi.org/10.1002/jgrd.50129

Swap R, Garstang M, Greco S, et al (1992) Saharan dust in the Amazon Basin. Tellus B 44B:133–149. https://doi.org/10.1034/j.1600-0889.1992.t01-1-00005.x

Taylor SR, McLennan SM (1995) The geochemical evolution of the continental crust. Rev Geophys 33:241. https://doi.org/10.1029/95RG00262

Tegen I, Schepanski K (2009) The global distribution of mineral dust. IOP Conf Ser Earth Environ Sci 7:012001. https://doi.org/10.1088/1755-1307/7/1/012001

Van de Velde K, Ferrari C, Barbante C, et al (1999) A 200 year record of atmospheric cobalt, chromium, molybdenum, and antimony in high altitude alpine firn and ice. Environ Sci Technol 33:3495–3501. https://doi.org/10.1021/es990066y

Vitousek PM, Walker LR (1989) Biological invasion by Myrica Faya in Hawai'i: Plant demography, nitrogen fixation, ecosystem effects. Ecol Monogr 59:247–265. https://doi.org/10.2307/1942601

Wang Y-P, Houlton BZ (2009) Nitrogen constraints on terrestrial carbon uptake: Implications for the global carbon-climate feedback. Geophys Res Lett 36:L24403. https://doi.org/10.1029/2009GL041009

Wolff E, Rankin A, Roethlisberger R (2003) An ice core indicator of Antarctic sea ice production? Geophys Res Lett 30:2158, doi: 10.1029/2003GL018454

Wurzburger N, Bellenger JP, Kraepiel AML, Hedin LO (2012) Molybdenum and phosphorus interact to constrain asymbiotic nitrogen fixation in tropical forests. PLoS One 7:1–7. https://doi.org/10.1371/journal.pone.0033710

Yu H, Chin M, Yuan T, et al (2015) The fertilizing role of African dust in the Amazon rainforest: A first multiyear assessment based on data from Cloud-Aerosol Lidar and

Infrared Pathfinder Satellite Observations. Geophys Res Lett 42:1984–1991. https://doi.org/10.1002/2015GL063040

Zender C, Miller R, Tegen I (2004) Quantifying Mineral Dust Mass Budgets: Terminology, Constraints, and Current Estimates. Eos (Washington DC) 85:509–512. https://doi.org/10.1029/2003JD003483

Zhang X, McRose DL, Darnajoux R, et al (2016) Alternative nitrogenase activity in the environment and nitrogen cycle implications. Biogeochemistry 127:189–198. https://doi.org/10.1007/s10533-016-0188-6

Figure legends

Figure 1. Annual sea-salt Mo sources (μg m^{-2} yr^{-1}) (a), Annual dust Mo sources (μg m^{-2} yr^{-1}) (b), Annual Mo sources from degassing volcanoes (μg m^{-2} yr^{-1}) (c).

Figure 2. Annual sea-salt Mo deposition (μg m^{-2} yr^{-1}) (a), Annual dust Mo deposition (μg m^{-2} yr^{-1}) with triangles indicating Bodélé dust samples and circles indicating Bodélé sediment samples (b), Annual Mo deposition from degassing volcanoes (μg m^{-2} yr^{-1}) (c), and combined annual sea-salt, dust, and volcano Mo deposition (μg m^{-2} yr^{-1}) with circles indicating where BNF studies have previously been conducted in the tropics, summarized in Supplementary Tables S2 and S3.

Figure 3. Locations of previous Mo addition experiments to free-living BNF mapped with annual natural Mo deposition (μg m^{-2} yr^{-1}). Blue circles indicate a free-living BNF response to Mo,

while red circles indicate no response of free-living BNF to Mo. Studies and locations are summarized in Supplementary Table S4.

Table legends

Table 1. Total Mo concentrations and sample locations for Bodélé Depression dust and sediment. Sample identification parameters correspond to those from Abouchami et al. (2013).

Table 2. Global sources of natural atmospheric Mo (Gg/yr) estimated from our model and by Ngiaru (1989).

Table 1. Total Mo concentrations and sample locations for Bodélé Depression dust and sediment. Sample identification parameters correspond to those from Abouchami et al. (2013).

Sample	Sample Description	Latitude	Longitude	Mo (μg g^{-1})
Bodélé Dust				
#1 Faya Largeau (Chad)		17° 56.113' N	19° 06.743'E	1.1
#1 Harmattan (Niamey, Niger)		13° 29.492' N	02° 10.189' E	1.2
#1 Radome (Niamey, Niger)		13° 29.492' N	02° 10.189' E	1.2
#2 Mao (rafters, Chad)		14° 07.704' N	15° 18.753' E	1.3
#2 Nguimi (police station, Chad)		14° 15.175' N	13° 06.878' E	1.0
Bodélé Sediment				
Bodéle soil 43.5 (Chad)	gray flakes and highly localized red plates	16° 06.120' N	18° 33.000' E	0.9
Bodéle soil 44 (Chad)	mixture of gray and white flakes of diatomite and surrounding sand	16 °08.139' N	18 °35.930' E	1.1
Bodéle soil 44B (Chad)	mixture of gray and white flakes of diatomite and surrounding sand	16 °08.139' N	18 °35.930' E	2.4
Bodéle soil 44C (Chad)	gray flakes and highly localized red plates	16 °12.273' N	18 °36.397' E	0.7
Bodéle soil 44D (Chad)	gray flakes and highly localized red plates	16 °12.273' N	18 °36.397' E	0.7
Bodéle soil 51 (Chad)	gray flakes and highly localized red plates	17 °13.777' N	19 °02.149' E	3.6
Bodéle soil 54A (Chad)	gray flakes and highly localized red plates	16 °09.190' N	18 °35.464' E	0.7
Bodéle soil 54B (Chad)	gray flakes and highly localized red plates	16 °09.190' N	18 °35.464' E	1.3

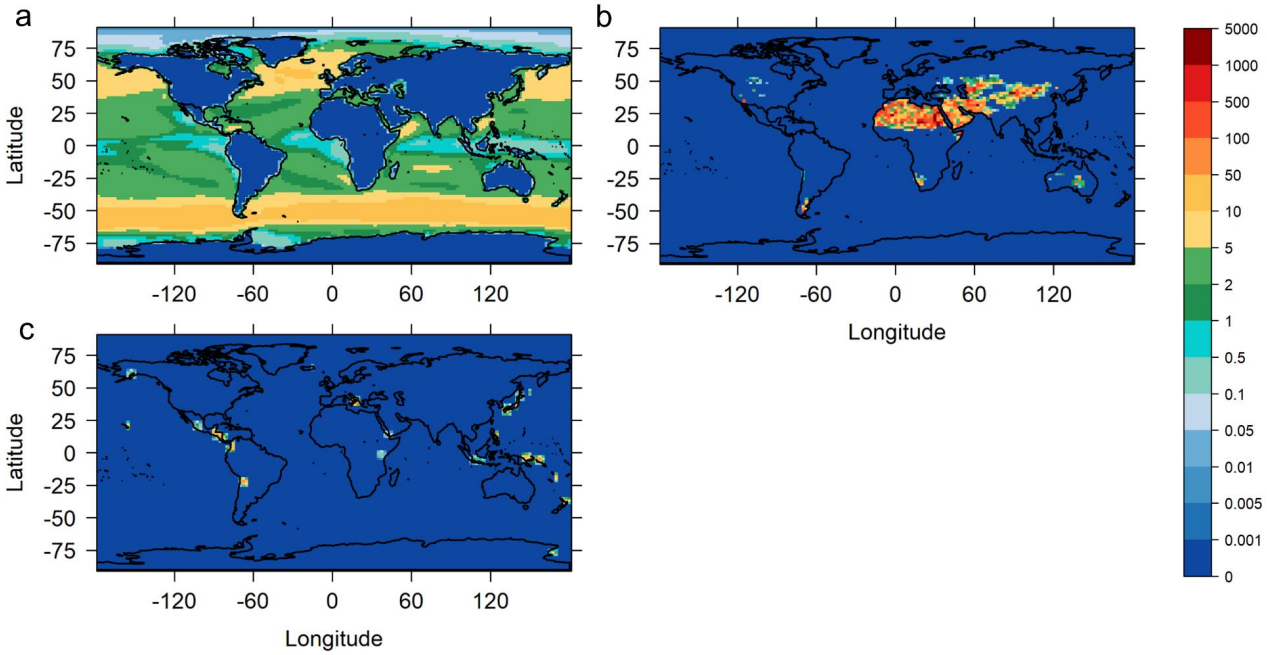

Figure 1. Annual sea-salt Mo sources (μg m^{-2} yr^{-1}) (a), Annual dust Mo sources (μg m^{-2} yr^{-1}) (b), Annual Mo sources from degassing volcanoes (μg m^{-2} yr^{-1}) (c).

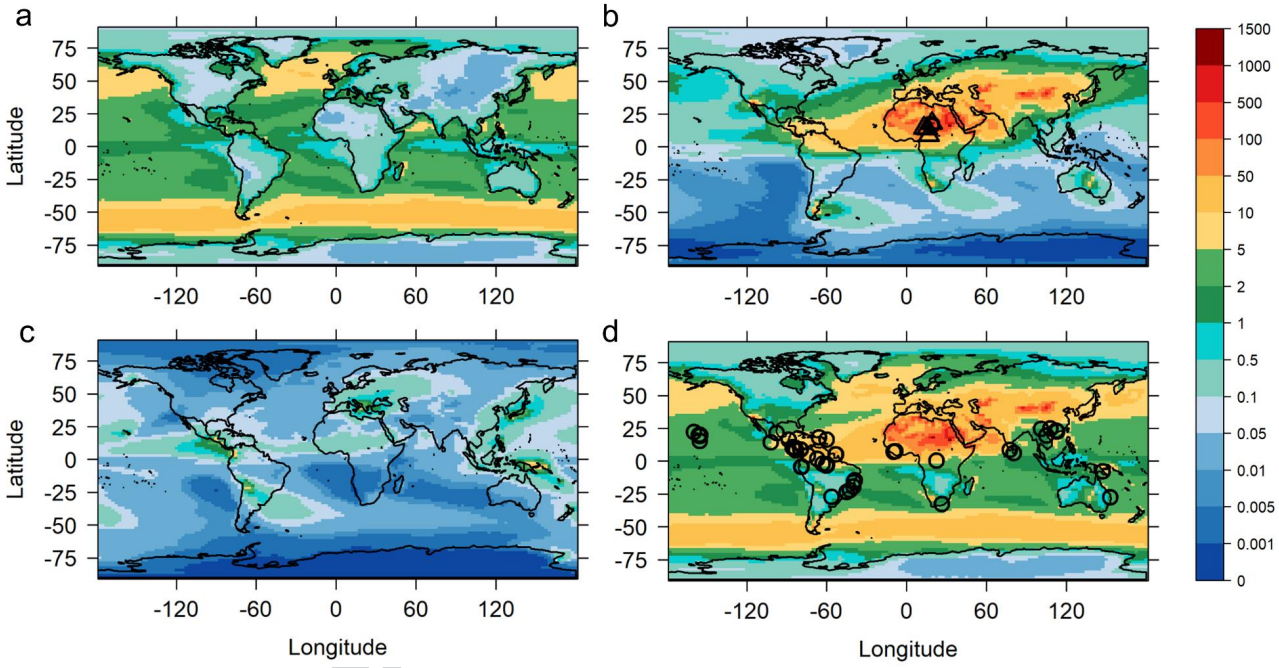

Figure 2. Annual sea-salt Mo deposition (μg m^{-2} yr^{-1}) (a), Annual dust Mo deposition (μg m^{-2} yr^{-1}) with triangles indicating Bodélé dust samples and circles indicating Bodélé sediment samples (b), Annual Mo deposition from degassing volcanoes (μg m^{-2} yr^{-1}) (c), and combined annual sea-salt, dust, and volcano Mo deposition (μg m^{-2} yr^{-1}) with circles indicating where BNF studies have previously been conducted in the tropics, summarized in Supplementary Tables S2 and S3.

Table 2. Global sources of natural atmospheric Mo (Gg/yr) estimated from our model and by Ngiaru (1989).

Source	Our Model	Ngiaru (1989)	Relative Uncertainty
Dust	4.3	1.3	Medium
Sea salts	1.6	0.22	Low
Volcanoes	0.22*	0.4	High

*Includes both degassing and eruptive volcanoes: 0.07 Gg/yr for degassing, and 0.15 Gg/yr for erupting volcanoes

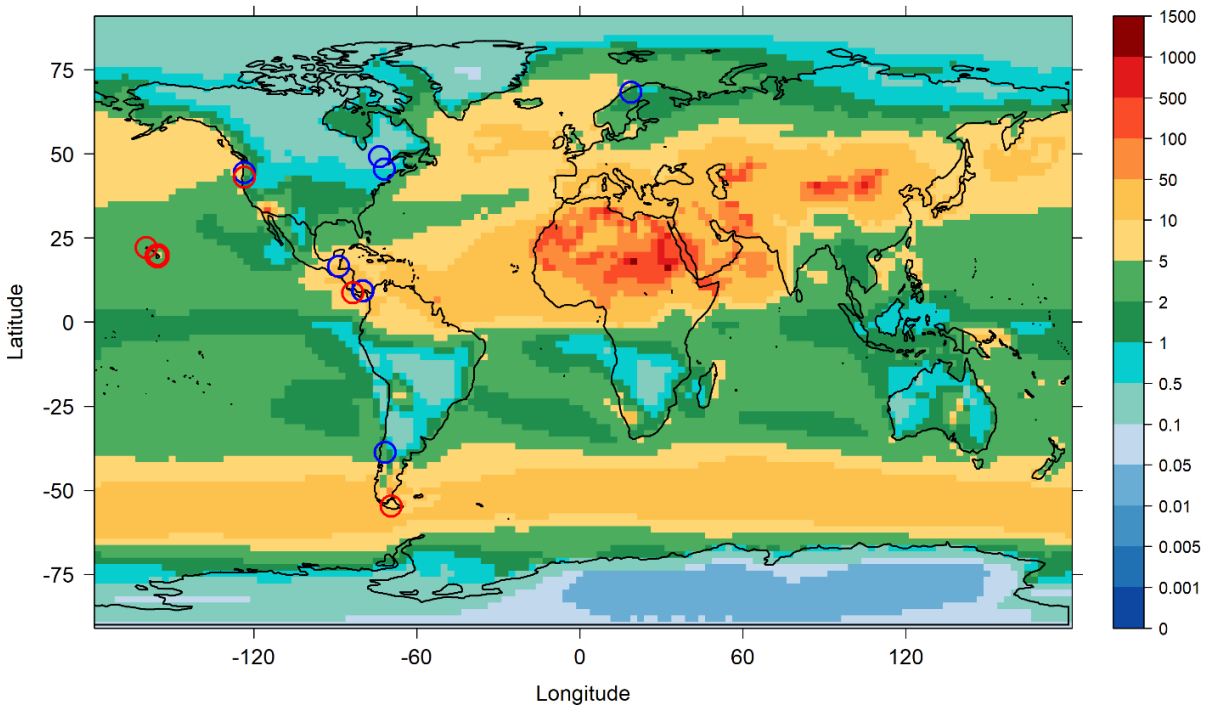

Figure 3. Locations of previous Mo addition experiments to free-living BNF mapped with annual natural Mo deposition (µg m-2 yr-1). Blue circles indicate a free-living BNF response to Mo, while red circles indicate no response of free-living BNF to Mo. Studies and locations are summarized in Supplementary Table S4.